

Cite this: *Dalton Trans.*, 2015, **44**, 14139

Dichlorodioxomolybdenum(vi) complexes bearing oxygen-donor ligands as olefin epoxidation catalysts†

Tânia S. M. Oliveira,^a Ana C. Gomes,^b André D. Lopes,^{*a} João P. Lourenço,^{a,c} Filipe A. Almeida Paz,^b Martyn Pillinger^b and Isabel S. Gonçalves^{*b}

Treatment of the solvent adduct $[\text{MoO}_2\text{Cl}_2(\text{THF})_2]$ with either 2 equivalents of *N,N*-dimethylbenzamide (DMB) or 1 equivalent of *N,N'*-diethyloxamide (DEO) gave the dioxomolybdenum(vi) complexes $[\text{MoO}_2\text{Cl}_2(\text{DMB})_2]$ (**1**) and $[\text{MoO}_2\text{Cl}_2(\text{DEO})]$ (**2**). The molecular structures of **1** and **2** were determined by single-crystal X-ray diffraction. Both complexes present a distorted octahedral geometry and adopt the *cis*-oxo, *trans*-Cl, *cis*-L configuration typical of complexes of the type $[\text{MoO}_2\text{X}_2(\text{L})_n]$, with either the monodentate DMB or bidentate DEO oxygen-donor ligands occupying the equatorial positions *trans* to the oxo groups. The complexes were applied as homogeneous catalysts for the epoxidation of olefins, namely *cis*-cyclooctene (Cy), 1-octene, *trans*-2-octene, α -pinene and (*R*)-(+)-limonene, using *tert*-butylhydroperoxide (TBHP) as oxidant. In the epoxidation of Cy at 55 °C, the desired epoxide was the only product and turnover frequencies in the range of ca. 3150–3200 mol mol_{Mo}⁻¹ h⁻¹ could be reached. The catalytic production of cyclooctene oxide was investigated in detail, varying either the reaction temperature or the cosolvent. Complexes **1** and **2** were also applied in liquid–liquid biphasic catalytic epoxidation reactions by using an ionic liquid of the type $[\text{C}_4\text{mim}][\text{X}]$ (C_4mim = 1-*n*-butyl-3-methylimidazolium; X = NTf₂, BF₄ or PF₆) as a solvent to immobilise the metal catalysts. Recycling for multiple catalytic runs was achieved without loss of activity.

Received 8th June 2015,
Accepted 29th June 2015
DOI: 10.1039/c5dt02165k

www.rsc.org/dalton

Introduction

Olefin epoxidation is an important reaction in organic synthesis due to the role of epoxides as intermediates in the manufacture of various industrial products, for example in the petroleum and plastics industries.¹ Since the beginning of studies on metal-based epoxidation catalysts, numerous types of molybdenum complexes have been synthesised and examined as catalysts or catalyst precursors.² In particular, dioxomolybdenum(vi) complexes of the type $[\text{MoO}_2\text{X}_2(\text{L})_n]$ with different anionic X (Cl, Br, F, alkyl, OR, OSiR₃, SR) and neutral L ligands have been widely investigated because they exhibit

excellent catalytic behaviour in olefin epoxidation using *tert*-butylhydroperoxide (TBHP) as oxidant.^{1–3} They have also been studied as oxo-transfer agents⁴ and as models for molybdoenzymes.⁵ The ligand(s) L may comprise one bidentate ligand with nitrogen,^{3,6} oxygen⁷ or sulfur⁸ donor atoms, or two monodentate ligands (e.g. DMF,⁹ THF,¹⁰ RCN,¹¹ R₂SO,¹² H₂O,^{12a,13} OPR₃^{7a,14}). Complexes formed with neutral bidentate ligands containing oxygen donor atoms have not attracted much attention, possibly due to the instability of the complexes. However, a limited number of studies hint at a promising catalytic behaviour for complexes containing *O*-ligands. For example, complexes of the type $[\text{MoO}_2\text{Cl}_2(\text{L})_2]$ bearing monodentate *N,N*-dialkylamide ligands have been shown to give high turnover frequencies in the range of 561–577 mol mol_{Mo}⁻¹ h⁻¹ for the epoxidation of *cis*-cyclooctene with TBHP, giving the epoxide as the only product in at least 98% yield after 6 h reaction at 55 °C.^{9e}

Herein, we describe two new complexes of the type $[\text{MoO}_2\text{Cl}_2(\text{L})_n]$ bearing *O*-donor ligands, one containing the monodentate ligand *N,N*-dimethylbenzamide (DMB), and another containing the bidentate ligand *N,N'*-diethyloxamide (DEO). To the best of our knowledge, the latter compound is the first example of a molybdenum(vi) complex bearing a

^aFaculty of Science and Technology, CIQA, University of the Algarve, Campus de Gambelas, 8005-136 Faro, Portugal. E-mail: adlopes@ualg.pt

^bDepartment of Chemistry, CICECO – Aveiro Institute of Materials, University of Aveiro, Campus Universitário de Santiago, 3810-193 Aveiro, Portugal.

E-mail: igoncalves@ua.pt

^cCQE – Centro de Química Estrutural, Instituto Superior Técnico, Av. Rovisco Pais, 1049-001 Lisboa, Portugal

† Electronic supplementary information (ESI) available: Olefin conversion kinetic profiles for complexes **2** and **3** (Fig. S1). CCDC 1057618 (**1**) and 1057619 (**2a**). For ESI and crystallographic data in CIF or other electronic format see DOI: 10.1039/c5dt02165k

neutral α -dicarbonyl ligand. The crystal structures of both complexes have been determined and a comprehensive study has been performed to assess their performance as catalysts for the epoxidation of olefins.

Experimental section

Materials and methods

Transmission FT-IR spectra were measured on a Mattson 7000 spectrometer with 128 scans and a resolution of 4.0 cm^{-1} . FT-Raman spectra were recorded on an RFS-100 Bruker FT-Spectrometer equipped with a Nd:YAG laser with an excitation wavelength of 1064 nm. ^1H NMR spectra were measured with a Bruker CXP 300 instrument. Chemical shifts are quoted in parts per million and referenced to tetramethylsilane.

All preparations and manipulations were carried out under nitrogen using standard Schlenk techniques. MoO_2Cl_2 (Sigma-Aldrich), anhydrous tetrahydrofuran (THF, 99.7%, Panreac), *N,N*-dimethylbenzamide (DMB, $\geq 98\%$, Alfa Aesar), *N,N'*-diethyloxamide (DEO, 98%, Alfa Aesar), acetonitrile (99.9%, Lab-Scan), *n*-hexane ($\geq 98.5\%$, Carlo Erba), diethyl ether (99.8%, Sigma-Aldrich), *cis*-cyclooctene (95%, Sigma-Aldrich), 1-octene (98%, Sigma-Aldrich), *trans*-2-octene (97%, Sigma-Aldrich), α -pinene (98%, Sigma-Aldrich), (*R*)-(+)-limonene (97%, Sigma-Aldrich), *n*-octane (98%, Merck-Schuchardt), undecane ($\geq 99\%$, Sigma-Aldrich), *tert*-butylhydroperoxide (5–6 M in decane, Sigma-Aldrich), benzotrifluoride (99%, Alfa Aesar), anhydrous 1,2-dichloroethane (99.8%, Sigma-Aldrich), ethanol (99.9%, Scharlau), and nitromethane ($>95\%$, Sigma-Aldrich) were purchased from commercial sources and used as received. The ionic liquids $[\text{C}_4\text{mim}][\text{Cl}]$, $[\text{C}_4\text{mim}][\text{BF}_4]$, $[\text{C}_4\text{mim}][\text{PF}_6]$ and $[\text{C}_4\text{mim}][\text{NTf}_2]$ were acquired from Solchemar and used as received. $[\text{MoO}_2\text{Cl}_2(\text{DMF})_2]$ (**3**) was synthesised according to the published procedure.^{9f,13a}

$[\text{MoO}_2\text{Cl}_2(\text{DMB})_2]$ (**1**)

After dissolving MoO_2Cl_2 (1.10 g, 5.53 mmol) in THF (15 mL), *N,N*-dimethylbenzamide (1.65 g, 11.06 mmol) was added and the mixture was stirred at room temperature for 1 h. The resultant pale yellow precipitate was isolated by filtration, washed with diethyl ether ($2 \times 15\text{ mL}$), and vacuum-dried. Yield: 2.51 g (91%). Anal. Calcd for $\text{C}_{18}\text{H}_{22}\text{Cl}_2\text{MoN}_2\text{O}_4$: C, 43.48; H, 4.46; N, 5.63. Found: C, 43.29; H, 4.54; N, 5.68%. FT-IR (KBr, cm^{-1}): $\nu = 3109$ (w), 3057 (w), 3035 (w), 2966 (w), 2935 (w), 1587 (vs), 1566 (vs), 1510 (s), 1475 (s), 1444 (s), 1404 (s), 1286 (w), 1265 (s), 1217 (w), 1180 (w), 1161 (w), 1147 (w), 1097 (m), 1078 (m), 1057 (m), 1024 (m), 1003 (w), 991 (w), 947 (vs, $\nu_{\text{sym}}(\text{Mo}=\text{O})$), 910 (vs, $\nu_{\text{asym}}(\text{Mo}=\text{O})$), 852 (m), 783 (s), 741 (s), 719 (s), 700 (s), 652 (s), 559 (m), 447 (m), 395 (s), 332 (vs, $\nu(\text{Mo}-\text{Cl})$). FT-Raman (cm^{-1}): $\nu = 3067$ (s), 2967 (w), 2939 (m), 2808 (w), 1601 (s), 1573 (w), 1514 (m), 1447 (m), 1414 (m), 1263 (w), 1217 (w), 1181 (w), 1162 (w), 1099 (w), 1025 (w), 1001 (s), 949 (vs), 910 (m), 782 (w), 741 (m), 725 (m), 651 (w), 615 (w), 561 (w), 447 (w), 397 (w), 347 (w), 322 (w), 302 (w), 259 (w), 207 (s), 144 (s), 107 (s). ^1H NMR (300 MHz, 298 K, CD_3CN): $\delta = 7.36$ (overlap-

ping signals, 10H), 3.01 (s, 6H), 2.88 (s, 6H). Single crystals of **1** suitable for X-ray diffraction were obtained by layering a solution of the complex in acetonitrile with a 1:1 mixture of hexane and diethyl ether, followed by storage of the mixture in the fridge for 24 h.

$[\text{MoO}_2\text{Cl}_2(\text{DEO})]$ (**2**)

After dissolving MoO_2Cl_2 (1.07 g, 5.38 mmol) in THF (15 mL), *N,N'*-diethyloxamide (0.775 g, 5.38 mmol) was added and the mixture was stirred at room temperature for 1 h. The resultant pale yellow precipitate was isolated by filtration, washed with diethyl ether ($2 \times 15\text{ mL}$), and vacuum-dried. Yield: 0.62 g (34%). Anal. Calcd for $\text{C}_6\text{H}_{12}\text{Cl}_2\text{MoN}_2\text{O}_4$: C, 21.01; H, 3.53; N, 8.17. Found: C, 20.81; H, 3.65; N, 8.24%. FT-IR (KBr, cm^{-1}): $\nu = 3330$ (vs, $\nu(\text{N}-\text{H})$), 3178 (m), 3107 (w), 3057 (w), 2983 (m), 2939 (w), 2881 (w), 1643 (vs), 1523 (s), 1462 (s), 1446 (s), 1388 (m), 1379 (m), 1350 (m), 1288 (m), 1267 (m), 1232 (m), 1151 (s), 1097 (m), 1041 (m), 955 (vs, $\nu_{\text{sym}}(\text{Mo}=\text{O})$), 912 (vs, $\nu_{\text{asym}}(\text{Mo}=\text{O})$), 741 (m), 673 (m), 565 (s), 507 (s), 391 (s), 337 (vs, $\nu(\text{Mo}-\text{Cl})$). FT-Raman (cm^{-1}): $\nu = 3337$ (w), 2981 (w), 2940 (s), 2878 (m), 1678 (w), 1636 (w), 1599 (m), 1554 (w), 1522 (w), 1447 (m), 1378 (s), 1332 (m), 1290 (w), 1267 (m), 1145 (w), 1058 (w), 1040 (w), 959 (vs), 913 (s), 803 (w), 505 (m), 390 (s), 316 (vs), 265 (s), 254 (s), 239 (vs), 192 (m), 140 (m). ^1H NMR (300 MHz, 298 K, CD_3CN): $\delta = 8.55$ (br, 2H), 3.54 (br, 4H), 1.26 (br, 6H). Single crystals (**2a**) suitable for X-ray diffraction were obtained by slow diffusion of diethyl ether into a solution of complex **2** in acetonitrile.

X-ray crystallography

The single crystals obtained upon recrystallisation of **1** and **2** (see above) were collected and immersed in highly viscous FOMBLIN Y perfluoropolyether vacuum oil (LVAC 140/13, Sigma-Aldrich) in order to prevent any possible degradation caused by the evaporation of the solvent.¹⁵ Crystals were mounted on a Hampton Research CryoLoop. Data were collected at 180(2) K on a Bruker X8 Kappa APEX II CCD area-detector diffractometer (Mo-K α graphite-monochromated radiation, $\lambda = 0.71073\text{ \AA}$) controlled by the APEX2 software package¹⁶ and equipped with an Oxford Cryosystems Series 700 cryostream monitored remotely using Cryopad.¹⁷ Images were processed using SAINT+,¹⁸ and data were corrected for absorption by the multiscan semi-empirical method implemented in SADABS.¹⁹ Structures were solved using the algorithm implemented in SHELXT-2014,²⁰ which allowed the immediate location of almost all of the heaviest atoms composing the molecular unit of the two compounds. The remaining missing non-hydrogen atoms were located from difference Fourier maps calculated from successive full-matrix least-squares refinement cycles on F^2 using the latest SHELXL from the 2014 release.²¹ All structural refinements were performed using the graphical interface ShelXle²² and all non-hydrogen atoms were refined assuming anisotropic displacement parameters.

The crystalline product obtained upon recrystallisation of **2** is referred to as **2a**. Besides the presence of two identical

complex molecular units in the asymmetric unit (*i.e.*, $Z' = 2$), the crystal structure determination for **2a** revealed the presence of an acetonitrile solvent molecule of crystallisation and one disordered, uncoordinated DEO molecule. One branch of this uncoordinated molecule was found to be disordered over two distinct crystallographic positions which were modelled into the final structure with rates of occupancy of 0.582(10) and 0.418(10), respectively.

Hydrogen atoms bound to carbon were placed at their idealised positions using appropriate *HFIX* instructions in SHELXL: 43 (aromatic carbon atoms), 23 (alkylic carbon atoms) or 137 (for the terminal methyl groups). These hydrogen atoms were included in subsequent refinement cycles with isotropic thermal displacement parameters (U_{iso}) fixed at 1.2 (for the two former families of hydrogen atoms) or $1.5 \times U_{\text{eq}}$ (solely for those associated with the methyl group) of the parent carbon atoms.

Hydrogen atoms associated with the amino groups of DEO molecules were directly located from difference Fourier maps. All these hydrogen atoms were included in the final structural model with the N–H distances restrained to 0.95(1) Å. The isotropic thermal displacement parameters (U_{iso}) of these hydrogen atoms were fixed at $1.5 \times U_{\text{eq}}$ of the parent nitrogen atoms.

The last difference Fourier map synthesis showed: for **1**, the highest peak (0.378 e \AA^{-3}) and deepest hole ($-0.528 \text{ e \AA}^{-3}$) located at 1.53 and 0.79 Å from H5 and Mo1, respectively; for **2a**, the highest peak (0.870 e \AA^{-3}) and deepest hole ($-0.739 \text{ e \AA}^{-3}$) located at 0.49 and 0.79 Å from H13A and Mo2, respectively. Structural drawings were created using Crystal Impact Diamond.²³ Information concerning crystallographic data collection and structure refinement details is summarised in Table 1.

Catalytic tests

The liquid-phase catalytic epoxidation of olefins was carried out with magnetic stirring (1100 rpm), under air, in closed borosilicate micro-reactors (5 mL) equipped with a valve to allow sampling. The reaction mixtures had a catalyst: substrate:TBHP ratio of 1:100:200. In typical runs, the following quantities were used: For **1**, 0.025 mmol of molybdenum complex, 2.5 mmol of olefin and 5.0 mmol of oxidant; for **2** and **3**, 0.035 mmol of molybdenum complex, 3.5 mmol of olefin and 7.0 mmol of oxidant.

The epoxidation of cyclooctene was performed without adding a cosolvent or by using 2 mL of benzotrifluoride (BTF), *n*-hexane, 1,2-dichloroethane (DCE), ethanol, acetonitrile or nitromethane. The mixture of olefin, TBHP and cosolvent (when used) was pre-heated to the reaction temperature in a temperature-controlled oil bath for 10 min, before adding the catalyst. The instant the catalyst was added was considered as time zero. Additional substrates (1-octene, *trans*-2-octene, α -pinene and (*R*)-(+)-limonene) were also studied, without the presence of a cosolvent.

Catalytic olefin epoxidation tests in the presence of ionic liquids (ILs) were carried out with exactly the same quantities

Table 1 Crystal and structure refinement data

	1	2a
Formula	C ₁₈ H ₂₂ Cl ₂ MoN ₂ O ₄	C ₂₀ H ₃₉ Cl ₄ Mo ₂ N ₇ O ₁₀
Formula weight	497.22	871.26
Temperature/K	180(2)	180(2)
Crystal system	Orthorhombic	Triclinic
Space group	<i>Fdd2</i>	<i>P1</i>
<i>a</i> /Å	16.9586(11)	9.6274(7)
<i>b</i> /Å	27.5327(19)	12.3705(9)
<i>c</i> /Å	8.5225(5)	16.4500(11)
α /°	90	96.854(3)
β /°	90	105.901(3)
γ /°	90	107.175(4)
Volume/Å ³	3979.3(4)	1756.9(2)
<i>Z</i>	8	2
<i>D_c</i> /g cm ⁻³	1.660	1.647
μ (Mo-K α)/mm ⁻¹	0.954	1.073
<i>F</i> (000)	2016	880
Crystal size/mm	0.20 × 0.10 × 0.08	0.16 × 0.14 × 0.11
Crystal type	Colourless blocks	Yellow plates
θ range	3.81 to 29.11	3.52 to 29.13
Index ranges	-23 ≤ <i>h</i> ≤ 23 -37 ≤ <i>k</i> ≤ 23 -11 ≤ <i>l</i> ≤ 11	-13 ≤ <i>h</i> ≤ 13 -16 ≤ <i>k</i> ≤ 16 -22 ≤ <i>l</i> ≤ 22
Reflections collected	8189	43 689
Independent reflections	2605 ($R_{\text{int}} = 0.0513$)	9428 ($R_{\text{int}} = 0.0358$)
Data completeness to $\theta = 25.24^\circ$	99.6%	99.7%
Data/restraints/parameters	2605/1/125	9428/19/442
Final <i>R</i> indices [$I > 2\sigma(I)$] ^{a,b}	$R_1 = 0.0331$ $wR_2 = 0.0705$	$R_1 = 0.0328$ $wR_2 = 0.0702$
Final <i>R</i> indices (all data) ^{a,b}	$R_1 = 0.0378$ $wR_2 = 0.0736$	$R_1 = 0.0427$ $wR_2 = 0.0754$
Weighting scheme ^c	$m = 0.0227$ $n = 2.3684$	$m = 0.0270$ $n = 1.3078$
Largest diff. peak and hole	0.378, -0.528 e Å ⁻³	0.870, -0.739 e Å ⁻³

$$^a R_1 = \sum ||F_o| - |F_c|| / \sum |F_o|. \quad ^b wR_2 = \sqrt{\sum [w(F_o^2 - F_c^2)^2] / \sum [w(F_o^2)^2]}.$$

$$^c w = 1/[\sigma^2(F_o^2) + (mP)^2 + nP] \text{ where } P = (F_o^2 + 2F_c^2)/3.$$

as those used in the tests without cosolvent, but with the addition of 0.5 mL of IL. The ILs studied were [C₄mim]Cl, [C₄mim]BF₄, [C₄mim]PF₆ and [C₄mim]NTf₂. For recycling, after the catalytic reaction the upper phase was removed from the reaction vessel with a Pasteur pipette. The IL phase was washed with *n*-hexane (with stirring). The upper phase was again removed with a Pasteur pipette and this operation was repeated 4 times. The organic phase was analysed by GC to check whether any TBHP, *n*-octane or cyclooctene oxide were still present. Additionally, oil pump vacuum for 30 min allowed the removal of *t*BuOH from the remaining IL phase before the next run. In the next run, the reaction time starts at the instant TBHP was added.

The catalytic reactions were monitored by gas chromatography (GC Bruker SCION 456-GC with a 30 m Macherey-Nagel OPTIMA delta-3 capillary column and a flame ionisation detector (FID)) using *n*-octane or undecane as internal standards. Samples were analysed without any further treatment. Samples that came from the catalytic experiments with ILs were taken after phase separation (stop stirring first).

Results and discussion

Synthesis and characterisation of the dioxomolybdenum(vi) complexes

Complexes **1** and **2** precipitated as pale yellow solids upon addition of DMB (2 equivalents) or DEO (1 equivalent) to a solution of the adduct $[\text{MoO}_2\text{Cl}_2(\text{THF})_2]$ in THF (Scheme 1). The compounds may be handled for short periods of time in air. Both complexes are soluble in ethanol, CH_3CN and CH_3NO_2 , and insoluble in BTF, *n*-hexane, DCE and diethyl ether.

The IR spectrum of **1** contains a pair of bands at 910 and 947 cm^{-1} (*cf.* 910 and 949 cm^{-1} in the Raman) which are assigned to the asymmetric and symmetric stretching vibrations of the *cis*- $[\text{MoO}_2]^{2+}$ group, respectively. The corresponding frequencies for the THF adduct $[\text{MoO}_2\text{Cl}_2(\text{THF})_2]$ are higher (*ca.* 960 and 920 cm^{-1}), consistent with the stronger coordination (*trans* to the oxo groups) of the amide ligand in **1**.^{9a,e} The donor capacity of the DMB ligand in **1** is, however, evidently lower than that for DMF in the complex $[\text{MoO}_2\text{Cl}_2(\text{DMF})_2]$ (**3**), which has the $\nu_{\text{sym}}(\text{Mo}=\text{O})$ band at about 940 cm^{-1} .^{9a} Complex **2** exhibits slightly higher frequencies (compared with **1**) for the $\nu(\text{Mo}=\text{O})$ modes (912 and 955 cm^{-1} in IR, 913 and 959 cm^{-1} in the Raman), possibly indicating an even lower donor capacity for the organic ligand and consequently a higher Lewis acidity for the metal centre. The IR spectra of **1** and **2** point to coordination of the organic ligands through the oxygen atom since the carbonyl stretching frequency shifts from 1626 and 1657 cm^{-1} for the free ligands DMB and DEO, respectively, to 1587 for **1** and 1643 cm^{-1} for **2**. This result is explained by the decrease in the double bond character of $\text{C}=\text{O}$ and the subsequent increase in the $\text{C}-\text{N}$ double bond character.^{9e} The smaller shift observed for **2** seems to be consistent with the weaker coordination of the ligand when compared with DMB in **1**.

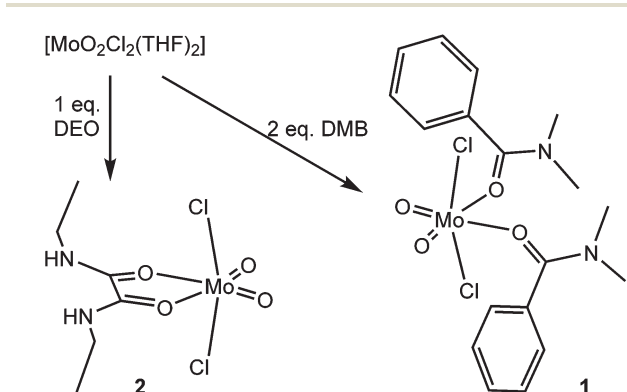
The ^1H NMR spectrum for complex **1** shows several overlapping signals centred at 7.36 ppm due to the hydrogen atoms of the phenyl ring, and two singlets at 2.88 and 3.01 ppm, one due to the methyl group *cis* to the carbonyl oxygen atom and the other due to the methyl group in the *trans* position. The

corresponding signals for the free ligand are shifted slightly downfield, appearing at 2.93 and 3.04 ppm. For complex **2**, the ^1H NMR spectrum shows broad signals at $\delta = 1.26$ (CH_3), 3.54 (CH_2) and 8.55 (NH).

Crystal structure description

The complexes $[\text{MoO}_2\text{Cl}_2(\text{DMB})_2]$ and $[\text{MoO}_2\text{Cl}_2(\text{DEO})]$ present in the crystalline compounds **1** and **2a** (Table 1) exhibit the expected structural features discussed above. While the crystal structure of **1** is solely composed of the individual discrete complexes, in **2a** the complex molecular units co-crystallised alongside solvent (acetonitrile) molecules and uncoordinated organic ligands.

In both compounds the Mo^{VI} centres are coordinated to two chlorine atoms, two terminal oxygen atoms, and two oxygen atoms from the organic ligand(s), which in **2a** appear as an *O,O'*-chelated molecule (Fig. 1 and 2). In both complexes the organic ligands form, alongside the terminal oxo groups, the equatorial plane of the distorted $\{\text{MoCl}_2\text{O}_4\}$ coordination polyhedra, with the chlorine atoms being positioned in the remaining apical positions. The terminal oxo groups in both complexes markedly exert the well-known *trans* effect with the $\text{Mo}=\text{O}$ bond lengths being found in the $1.681(3)$ – $1.6901(18)\text{ \AA}$ range, which contrast with the longer $\text{Mo}-\text{O}$ bonds to the organic ligands, $2.2157(15)$ – $2.2394(16)\text{ \AA}$ (Tables 2 and 3). The longer $\text{Mo}-\text{Cl}$ bond distances, allied with the large dispersion in the *cis* and *trans* internal octahedral angles [$70.76(5)$ – $105.14(10)^\circ$ and $159.76(3)$ – $168.15(16)^\circ$, respectively], further demonstrate the highly distorted coordination environment for all Mo^{VI} centres.



Scheme 1 Preparation of **1** and **2**. Reaction conditions: THF, RT, 1 h.

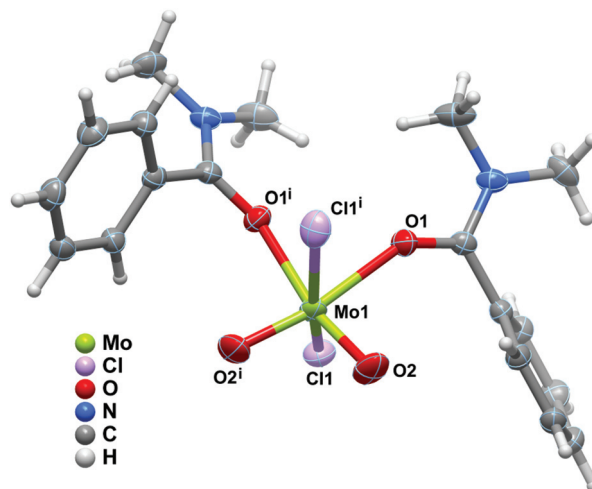


Fig. 1 Schematic representation of the molecular unit composing the crystal structure of **1**. Non-hydrogen atoms are represented as thermal ellipsoids drawn at the 50% probability level and hydrogen atoms as small spheres with arbitrary radii. For simplicity, only the atoms composing the first coordination sphere of the crystallographically independent molybdenum centre are labelled. Symmetry transformation used to generate equivalent atoms: (i) $1-x, 1-y, z$.

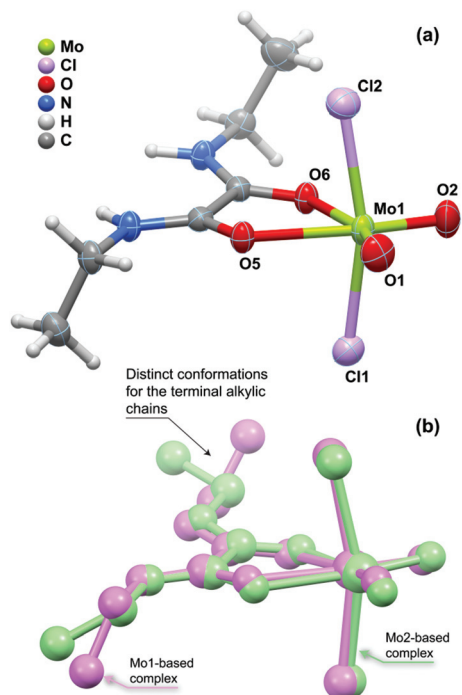


Fig. 2 (a) Schematic representation of one independent molecular unit composing the crystal structure of **2a**. Please see the caption to Fig. 1 for general comments about the graphical representation. (b) Overlay of the two crystallographically independent $[\text{MoO}_2\text{Cl}_2(\text{DEO})]$ complexes composing the asymmetric unit in **2a** (hydrogen atoms have been omitted for clarity), emphasising the distinct conformations for the terminal alkylic chains of the organic ligands.

Table 2 Selected bond lengths (in Å) and angles (in degrees) for the crystallographically independent molybdenum centre present in compound $[\text{MoO}_2\text{Cl}_2(\text{DMB})_2]$ (**1**)^a

Mo1–O1	2.219(3)	Mo1–O2i	1.681(3)
Mo1–O1i	2.219(3)	Mo1–Cl1	2.3800(12)
Mo1–O2	1.681(3)	Mo1–Cl1i	2.3800(12)
O1–Mo1–O1i	77.82(15)	O2i–Mo1–O1	168.15(16)
O1–Mo1–Cl1	81.98(8)	O2i–Mo1–O1i	90.45(14)
O1–Mo1–Cl1i	82.52(8)	O2i–Mo1–O2	101.3(2)
O1i–Mo1–Cl1	82.52(8)	O2i–Mo1–Cl1	94.92(14)
O1i–Mo1–Cl1i	81.98(8)	O2–Mo1–Cl1i	94.93(14)
O2–Mo1–O1	90.45(14)	O2i–Mo1–Cl1i	97.69(14)
O2–Mo1–O1i	168.15(16)	Cl1–Mo1–Cl1i	160.04(6)
O2–Mo1–Cl1	97.69(14)		

^a Symmetry transformation used to generate equivalent atoms: (i) $1 - x, 1 - y, z$.

In compound **2a**, as mentioned above, the asymmetric unit is composed of two identical $[\text{MoO}_2\text{Cl}_2(\text{DEO})]$ complexes (Fig. 2b). The configuration of the complexes is, nevertheless, identical, apart from conformational differences regarding the terminal alkylic chains of the DEO ligand.

Catalytic epoxidation

The epoxidation of *cis*-cyclooctene using complexes **1**, **2** and **3** as catalyst precursors at 55 °C, with no solvent added other

Table 3 Selected bond lengths (in Å) and angles (in degrees) for the two crystallographically independent molybdenum centres present in **2a**

Mo1–O1	1.6847(17)	Mo1–O6	2.2186(14)
Mo1–O2	1.6888(17)	Mo1–Cl1	2.3726(6)
Mo1–O5	2.2259(15)	Mo1–Cl2	2.3853(7)
O1–Mo1–O2	104.89(9)	O2–Mo1–Cl2	95.77(7)
O1–Mo1–O5	90.72(7)	O5–Mo1–Cl1	82.86(4)
O1–Mo1–O6	161.32(8)	O5–Mo1–Cl2	83.47(4)
O1–Mo1–Cl1	95.84(7)	O6–Mo1–O5	70.76(5)
O1–Mo1–Cl2	95.26(7)	O6–Mo1–Cl1	84.57(4)
O2–Mo1–O5	164.36(7)	O6–Mo1–Cl2	80.59(4)
O2–Mo1–O6	93.68(7)	Cl1–Mo1–Cl2	162.47(2)
O2–Mo1–Cl1	94.43(7)		
Mo2–O3	1.6901(18)	Mo2–O8	2.2157(15)
Mo2–O4	1.6823(18)	Mo2–Cl3	2.3669(8)
Mo2–O7	2.2394(16)	Mo2–Cl4	2.3673(8)
O3–Mo2–O7	91.42(8)	O4–Mo2–Cl4	95.37(7)
O3–Mo2–O8	162.35(8)	O7–Mo2–Cl3	81.30(5)
O3–Mo2–Cl3	97.33(8)	O7–Mo2–Cl4	82.98(5)
O3–Mo2–Cl4	95.73(8)	O8–Mo2–O7	71.11(6)
O4–Mo2–O3	105.14(10)	O8–Mo2–Cl3	82.89(5)
O4–Mo2–O7	163.44(8)	O8–Mo2–Cl4	80.01(5)
O4–Mo2–O8	92.35(8)	Cl3–Mo2–Cl4	159.76(3)
O4–Mo2–Cl3	96.07(7)		

than the decane present in the TBHP solution, yielded cyclooctene oxide (CyO) as the only reaction product (Fig. 3 and Table 4). Complex **3** has been previously studied in this reaction (although under different conditions from those used here),^{9f} and was used in this work as a reference.

Fig. 3 displays the conversion of *cis*-cyclooctene obtained at selected reaction times for the complexes studied. The data reveal the outstanding catalytic activity of **1** and **2** under the reaction conditions used, with a nearly full conversion being reached at 2 min reaction time, the first point evaluated.

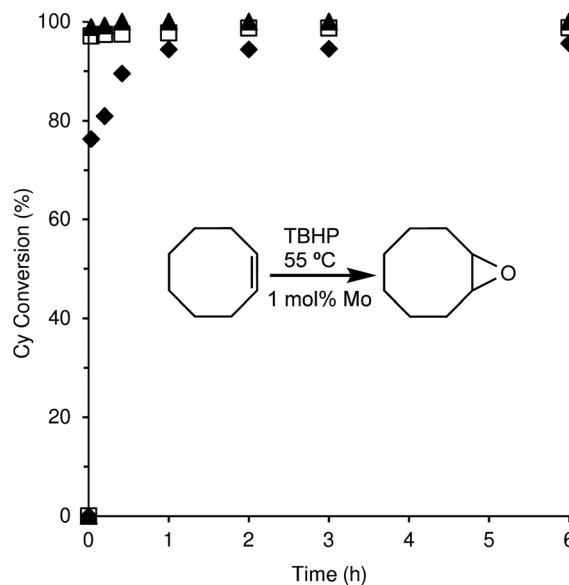


Fig. 3 Kinetic profiles of the catalytic epoxidation of *cis*-cyclooctene (Cy) using **1** (□), **2** (▲) and **3** (◆) as catalyst precursors, without cosolvent.

When compared with complex **3**, which had already been shown to be an excellent catalyst for this reaction,^{9f} a much higher conversion is obtained with **1** and **2** in the early stages of the reaction, although a similar catalytic performance is observed for longer reaction times. It is expected, based on previous studies of [MoO₂X₂(L)_n]-type complexes,^{6c,k,9e,f} that the initial complexes act as pre-catalysts, forming the active species in the reaction medium. Therefore, the data obtained may suggest that the formation of the active species is faster for complexes **1** and **2** than for complex **3**. On the other hand, the FT-IR data discussed above suggest that the ligands DMB (complex **1**) and DEO (complex **2**) have less donating character than DMF (complex **3**), which may give rise to a more acidic metal centre in both complexes that could also contribute to a higher activity of the active species. The turnover frequency (TOF) values obtained at 2 min reaction time (Table 4) are strikingly high for all three catalysts (in the range of 2500–3200 mol mol_{Mo}⁻¹ h⁻¹), which probably reflects the same type of active species and reaction mechanism. Table 5 compares the results obtained in the epoxidation of *cis*-cyclooctene with complexes **1**–**3** with values found in the literature for complexes with similar characteristics, namely dichlorodioxomolybdenum(vi) complexes bearing monodentate ligands which coordinate to the metal through an oxygen atom.

The epoxidation of other olefins, namely 1-octene, *trans*-2-octene, α -pinene and (*R*)-(+)-limonene, was also studied for complexes **1**, **2** and **3**, without cosolvent at 55 °C (Table 4, Fig. 4 for complex **1** and Fig. S1 in the ESI† for complexes **2** and **3**). The data obtained clearly show that under these experi-

mental conditions the catalytic performance of complex **2**, when compared with that of complex **1**, is always higher at the early stages of the reaction and independent of the type of olefin used as substrate. These differences in catalytic behaviour point to the key role of the rate of formation of the active species in the catalytic process, as suggested above. The comparison of the three complexes in terms of initial TOF numbers and kinetic profile shows that the relative catalytic behaviour is the same for cyclooctene, α -pinene and limonene, but quite different for the linear olefins 1-octene and *trans*-2-octene. For these cases, complex **3** shows higher initial activity than complex **1**. The reason for this fact is not clear at this point but the influence of steric effects cannot be discarded.

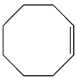
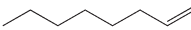
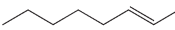
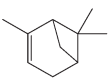
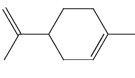
The study of the epoxidation of the structurally different olefins has shown that the three complexes behave in a similar way. The catalytic activity is in accordance with the increasing presence of alkyl groups that increase the electron density at the double bond, *i.e.*, 1-octene < *trans*-2-octene < α -pinene < limonene < *cis*-cyclooctene, as expected for catalytic systems involving these types of catalysts.^{9e,f}

Concerning selectivity, for all three complexes the reaction of 1-octene and *trans*-2-octene gave, respectively, 1,2-epoxyoctane and 2,3-epoxyoctane as the only reaction products. On the other hand, and despite the significant conversions obtained for both α -pinene and (*R*)-(+)-limonene, the selectivities to the corresponding epoxides were rather low. For α -pinene, the selectivity to the epoxide was below 5% for all the catalysts under study, and several byproducts were obtained that included campholenic aldehyde. In the case of (*R*)-(+)-limonene, the reaction also originated a wide variety of compounds that included limonene oxide and carvone as the main products. Nevertheless, no products were identified that could indicate the epoxidation of the terminal double bond, which agrees with the results found for the linear olefins 1-octene and *trans*-2-octene where the more electron-rich double bond of *trans*-2-octene is more easily oxidised.

The influence of an additional solvent in the reaction medium was investigated using *cis*-cyclooctene as model substrate (Fig. 5 and Table 6). The catalytic tests were carried out at 35 °C due to the high activity of the complexes at 55 °C that might mask any solvent-dependent differences. Data in Table 6 also give complementary information on the influence of the temperature on the catalytic activity. For all the complexes, the TOF values and the conversion of *cis*-cyclooctene are, as expected, significantly lower than those obtained at 55 °C. Depending on the type of solvent used, benzotrifluoride (BTF), *n*-hexane, 1,2-dichloroethane (DCE), ethanol, CH₃CN or CH₃NO₂, the catalytic results changed significantly, although with no effect on the selectivity to the epoxide which was always 100%.

Nitromethane is a polar solvent and in spite of the dilution effect caused by its addition to the reaction medium, its use is beneficial in all cases since the reaction rate increases significantly when compared with the reaction carried out in the absence of an additional solvent or with other solvents tested.

Table 4 Catalytic performance of complexes **1**, **2** and **3** in the epoxidation of *cis*-cyclooctene, 1-octene, *trans*-2-octene, α -pinene, and (*R*)-(+)-limonene, using TBHP at 55 °C

Olefin	Cat.	TOF ^a (mol mol _{Mo} ⁻¹ h ⁻¹)	Conv. ^b (%)	Select. ^b (%)
	1	3199	99/100	100/100
	2	3149	100/100	100/100
	3	2499	96/100	100/100
	1	41	32/62	100/100
	2	182	51/70 ^c	100/100
	3	107	33/64 ^c	100/100
	1	91	70/91 ^c	100/100
	2	208	67/86 ^c	100/100
	3	239	56/85	100/100
	1	1268	55/70 ^c	4/2 ^d
	2	1527	55/81 ^c	5/3 ^d
	3	581	51/61	4/5 ^d
	1	1162	93/97	33/19; 37/12 ^e
	2	2414	96/99	33/21; 22/16 ^e
	3	557	96/98	20/32; 7/12 ^e

^a Turnover frequency calculated at 2 min reaction. ^b Cyclooctene conversion and selectivity to epoxide after 6/24 h reaction, unless indicated otherwise. ^c 3/24 h reaction. ^d Other products were formed which were not identified. ^e Selectivity to carvone (other products were formed which were not identified).

Table 5 Epoxidation of *cis*-cyclooctene at 55 °C with TBHP (in decane) and different molybdenum complexes as catalyst precursors

Complex ^a	Mo : Cy : TBHP	Cosolvent ^b	TOF ^c	Ref.
1	1 : 100 : 200	ns	3199 (2)	This work
2	1 : 100 : 200	ns	3149 (2)	This work
3	1 : 100 : 200	ns	2499 (2)	This work
[MoO ₂ Cl ₂ (DMF) ₂]	1 : 100 : 160	ns	1003 (10)	9f
[MoO ₂ Cl ₂ (OPMePh ₂) ₂]	1 : 100 : 150	ns	150 (30)	7a
[MoO ₂ Cl ₂ dppmO ₂]	1 : 100 : 150	ns	71 (30)	7a
[MoO ₂ Cl ₂ (DPF) ₂]	1 : 100 : 150	ns	575 (10)	9e
[MoO ₂ Cl ₂ (DPF) ₂]	1 : 100 : 150	DCE	605 (10)	9e

^a OPMePh₂ = methyl(diphenyl)phosphine oxide; dppmO₂ = bis(diphenylphosphineoxide)methane; DPF = *N,N*-diphenylformamide. ^b ns = no cosolvent was added. ^c TOF (mol mol_{Mo}⁻¹ h⁻¹). The reaction time used to calculate the TOF is given in parentheses. For all systems the Cy conversion at 24 h was 100%.

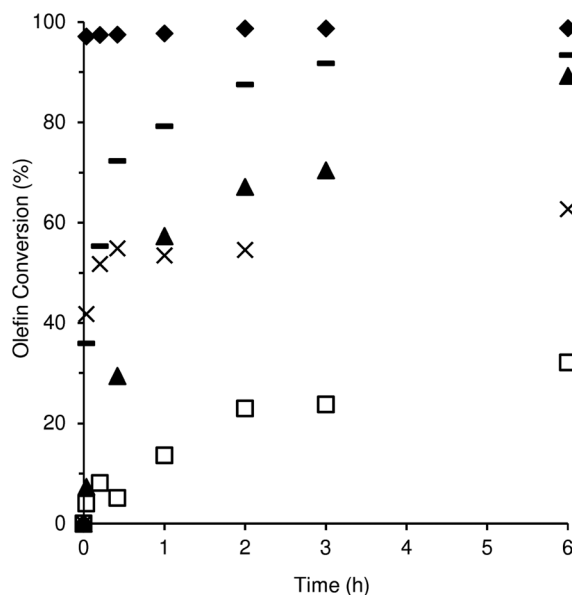


Fig. 4 Oxidation of *cis*-cyclooctene (◆), 1-octene (□), *trans*-2-octene (▲), α -pinene (×) and (*R*)-(+)-limonene (—) with TBHP using complex 1 as catalyst precursor at 55 °C, without cosolvent.

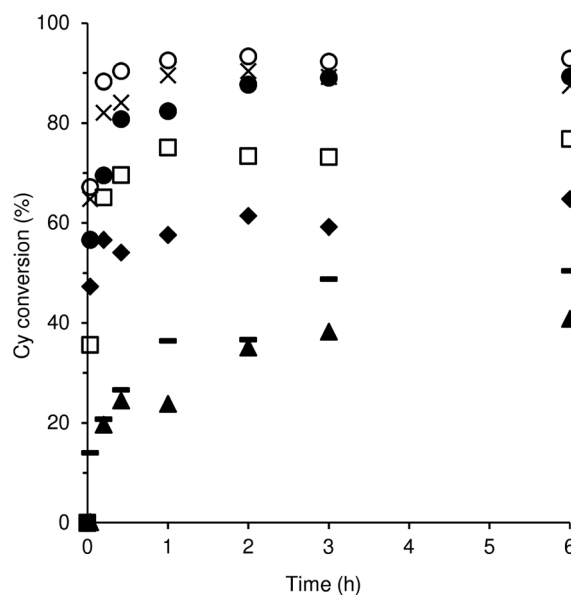


Fig. 5 Kinetic profiles of *cis*-cyclooctene epoxidation in the presence of 2, using TBHP at 35 °C without a cosolvent (◆), or with BTF (□), *n*-hexane (▲), DCE (×), ethanol (—), CH₃CN (●) or CH₃NO₂ (○) as cosolvents.

The low catalytic activity obtained in presence of *n*-hexane, non-polar and aprotic, may be explained by the low solubility of the complexes in this solvent that will give rise to a small amount of active species in the reaction medium. Data in Table 6 are therefore significantly influenced by the dielectric properties of the solvent, probably due to changes in the solubilities of the complexes.

CH₃NO₂ has similar characteristics in terms of dielectric constant to CH₃CN but gives rise to higher catalytic activity. This behaviour is probably related with the coordinating properties of CH₃CN that allow the participation of solvent molecules in the catalytic process, causing a decrease in activity. In fact, the use of ethanol, another polar and coordinating solvent, give rise to an even lower catalytic activity when compared with polar and non-coordinating solvents such as CH₃NO₂, BTF and DCE.

With the aim of studying the catalytic behaviour of these dioxomolybdenum(vi) complexes in a biphasic system, epoxidation of *cis*-cyclooctene was carried out in the presence of different ionic liquids (IL). Such biphasic systems may have implications on the stability of the active species since the complex is dissolved in the IL phase, and additionally may simplify the recycling procedure.

Table 7 shows the catalytic data obtained with the complexes 1 and 2 at 55 °C. Data for [C₄mim][Cl] are not shown since this IL did not allow a phase separation and, additionally, no catalytic activity could be observed. For the remaining ILs a complete phase separation was achieved and both complexes showed significant activity with 100% selectivity to the epoxide. When compared with the system in the absence of any solvent (Table 4), both complexes show a decrease in

Table 6 Catalytic performance of complexes **1**, **2** and **3** in the epoxidation of *cis*-cyclooctene^a

Catalyst	Cosolvent ^b	TOF ^c (mol mol _{M₀} ⁻¹ h ⁻¹)	Conv. ^d (%)
1	None	1680	68/84
	Hexane (1.89)	114	47/52
	BTF (9.18)	1597	83/90
	DCE (10.4)	2601	94/98
	EtOH (24.6)	887	42/66
	CH ₃ NO ₂ (35.9)	2885	97/99
2	CH ₃ CN (36.6)	1274	82/85
	None	1496	65/76
	Hexane	3	41/54
	BTF	1148	77/92
	DCE	2111	88/94
	EtOH	457	50/80
3	CH ₃ NO ₂	2152	93/97
	CH ₃ CN	1790	89/93
	None	1666	77/86
	Hexane	161	47/55
	BTF	1320	79/91
	DCE	2013	93/96
EtOH	83	45/78	
CH ₃ NO ₂	2692	97/98	
CH ₃ CN	885	85/91	

^a Reaction conditions: 35 °C, catalyst/substrate/TBHP molar ratio = 1 : 100 : 200. ^b Dielectric constants are given in parentheses. ^c Turnover frequency calculated at 2 min reaction. ^d Cyclooctene conversion after 6/24 h reaction.

Table 7 Epoxidation of *cis*-cyclooctene in the presence of ionic liquids

Catalyst	Ionic liquid	TOF ^a (mol mol _{M₀} ⁻¹ h ⁻¹)	Conv. ^b (%)
1	[C ₄ mim][NTf ₂]	2914	100/100
	[C ₄ mim][BF ₄]	2572	98/100
	[C ₄ mim][PF ₆]	2899	96/96
2	[C ₄ mim][NTf ₂]	1913	87/97
	[C ₄ mim][BF ₄]	1849	93/93
	[C ₄ mim][PF ₆]	1967	70/71

^a Turnover frequency calculated at 2 min reaction. ^b Cyclooctene conversion after 6/24 h reaction.

activity at the early stages of the reaction, reflected in the lower values of TOFs obtained. This was expected due to the biphasic nature of the system, with the catalyst and *cis*-cyclooctene in different phases.

Table 8 Recycling runs with *cis*-cyclooctene

Catalyst/IL	Run 1		Run 2		Run 3		Run 4	
	TOF ^a	Conv. ^b	TOF ^a	Conv. ^b	TOF ^a	Conv. ^b	TOF ^a	Conv. ^b
1/[C ₄ mim][NTf ₂]	2914	99	2041	99	2217	99	2464	100
2/[C ₄ mim][NTf ₂]	1913	87	1011	99	3031	100	2252	100
2/[C ₄ mim][BF ₄]	1849	93	846	72	594	95	690	92

^a Turnover frequency (mol mol_{M₀}⁻¹ h⁻¹) calculated at 2 min reaction. ^b Cyclooctene conversion after 2 h reaction for complex **1** and 4 h reaction for complex **2**.

The behaviour of the catalytic system is clearly influenced both by the nature of the anionic part of the IL and by the complex. Comparing complex **1** with complex **2**, the data show that the catalytic activity of complex **1** is higher at the early stages of the reaction and does not seem to change with the nature of the IL. A similar behaviour in terms of activity of complexes **1** and **2** was already encountered in the presence of cosolvents at 35 °C. Thus, decreasing the reaction rate, either by addition of a solvent, lowering the temperature or addition of an IL, emphasises different rates of formation of active species between the catalysts. The formation of the active species may involve the loss or substitution of ligands and further work is in progress in order to clarify this important issue. Concerning the conversion it is also clear that complex **1** is more active than complex **2**, in line with the TOF values obtained at the beginning of the reaction.

Comparing the different ILs, higher conversions at 24 h are obtained with the IL comprising NTf₂⁻ as anionic part followed by the one with BF₄⁻ and finally the IL with PF₆⁻ counter-ions. This behaviour is observed for both complexes but is more evident for complex **2**, probably due to the lower reaction rate. The data suggest that the anionic part of the IL may have an influence on the catalytically active species. In fact, the interaction of the NTf₂⁻ anion has already been proposed for a palladium(II) complex.²⁴ Illner *et al.* even referred that the small interaction observed for one of their complexes may raise the question of whether the coordination to the metal centre might be possible at a very large excess of this anion (for example, on dissolving the complex in an ionic liquid) in spite of its low nucleophilicity.

The catalytic systems containing the ILs allow a complete and fast phase separation once the stirring is stopped, and therefore offer the opportunity to devise a simple and effective recycling procedure. In order to evaluate the stability of these catalysts during consecutive runs, several recycling experiments were undertaken. Catalysts **1** and **2** were tested with [C₄mim][NTf₂], and catalyst **2** was also tested with [C₄mim][BF₄]. The results in Table 8 for the IL [C₄mim][NTf₂] indicate that the active species are stable in the reaction media and that the catalysts are dissolved in the IL phase since no loss of activity is observed in consecutive runs.

Surprisingly, the activity of the catalysts seems to increase with the consecutive runs when [C₄mim][NTf₂] is used. This is

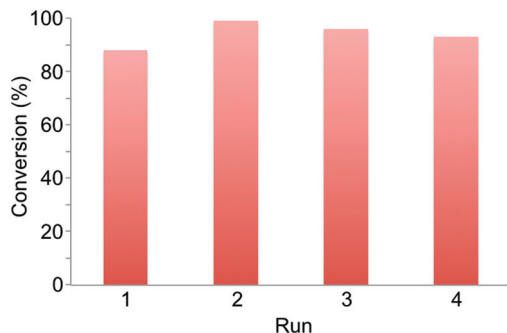


Fig. 6 Olefin conversion with complex 2 and $[C_4mim][NTf_2]$. Runs 1 and 2 correspond to the epoxidation of *cis*-cyclooctene, and runs 3 and 4 correspond to the epoxidation of (*R*)-(+)-limonene.

more evident with catalyst 2, probably due to its lower catalytic activity. For this catalyst the conversion obtained after 4 h in the first run is only 87%. However, in the following runs, the conversions are 99–100%, indicating a progressive increase in activity. Although the present data do not allow a full comprehension of the reasons behind this behaviour, as mentioned before, the participation of the NTf_2^- ion in the stabilisation of the active species cannot be discarded at this point. It should be noted that the initial reaction rates are necessarily lower in the second and following runs when compared with the first run due to the fact that the reaction is initiated with the addition of TBHP, which is at room temperature and therefore colder than the reaction media.

Due to the exceptional stability of the catalytic species and the simplicity of the recycling procedure, the possibility of changing the olefin between recycling cycles was also tested. The system comprising catalyst 2 and $[C_4mim][NTf_2]$ was used to convert *cis*-cyclooctene for 2 cycles and then the olefin was changed and the system used to convert limonene for 2 more cycles. The results in Fig. 6 clearly show that the system is highly robust and flexible, opening up a wide range of applications.

Conclusions

Two new complexes of the type $[MoO_2Cl_2(L)_n]$ bearing oxygen-donor ligands have been prepared and characterised. To the best of our knowledge, complex 2 containing bidentate DEO is the first example of a dioxomolybdenum(vi) complex with a neutral α -dicarbonyl ligand. These complexes are extremely active and selective catalysts for the epoxidation of standard substrates such as *cis*-cyclooctene, using TBHP as oxidant. The enhanced Lewis acidity of the complexes probably contributes in a major way to their high catalytic activity. On the other hand, this high acidity may explain the lower selectivities measured for more sensitive epoxides such as α -pinene oxide and limonene oxide. Complexes 1 and 2 were also applied in liquid–liquid biphasic catalytic epoxidation reactions by using an ionic liquid as a solvent to immobilise the metal catalysts.

The reaction products (cyclooctene oxide and *t*BuOH) could be efficiently removed by extraction and evaporation steps, and the resultant IL–catalyst mixture could be recycled for multiple catalytic runs without loss of activity, suggesting that the dissolved catalyst was stable and resistant to leaching. Moreover, we have shown that a regenerated IL–catalyst mixture can be successfully reused with a different substrate from that used initially. Of the four different ILs examined in this study (changing only the nature of the counter-anion), the best results were obtained with $[C_4mim][NTf_2]$. The NTf_2^- anion could play a non-innocent role, interacting with Mo^{VI} centres. To gain further insight into the chemistry of these systems and to optimise the catalytic process, future work should focus on a systematic investigation of a wider range of imidazolium-based ILs, varying not only the anion but also the cation.

Acknowledgements

We acknowledge funding by FEDER (Fundo Europeu de Desenvolvimento Regional) through COMPETE (Programa Operacional Factores de Competitividade). National funding through the FCT (Fundação para a Ciência e a Tecnologia) within the projects FCOMP-01-0124-FEDER-029779 (FCT ref. PTDC/QEQ-SUP/1906/2012, including research grants to A.C.G. (ref. BPD/UI89/4864/2014) and T.S.M.O.) and FCOMP-01-0124-FEDER-020658 (FCT ref. PTDC/EQU-EQU/121677/2010) is thanked. This work was developed in the scope of the project CICECO – Aveiro Institute of Materials (FCT ref. UID/CTM/50011/2013), financed by national funds through the FCT/MEC and co-financed by FEDER under the PT2020 Partnership Agreement. The FCT and CICECO are acknowledged for financial support towards the purchase of the single-crystal diffractometer.

Notes and references

- (a) M. G. Clerici, M. Ricci and G. Strukul, in *Metal-catalysis in Industrial Organic Processes*, ed. G. P. Chiusoli and P. M. Maitlis, Royal Society of Chemistry Publishing, Cambridge, 2008; (b) K. Jeyakumar and D. K. Chand, *J. Chem. Sci.*, 2009, **121**, 111.
- R. Sanz and M. R. Pedrosa, *Curr. Org. Synth.*, 2009, **6**, 239.
- (a) F. E. Kühn, A. M. Santos, I. S. Gonçalves, C. C. Romão and A. D. Lopes, *Appl. Organomet. Chem.*, 2001, **15**, 43; (b) F. E. Kühn, A. M. Santos and M. Abrantes, *Chem. Rev.*, 2006, **106**, 2455; (c) K. R. Jain, W. A. Herrmann and F. E. Kühn, *Coord. Chem. Rev.*, 2008, **252**, 556.
- F. J. Arnáiz, R. Aguado and J. M. Martínez de Ilduya, *Polyhedron*, 1994, **13**, 3257.
- J. H. Enemark, J. J. A. Cooney, J.-J. Wang and R. H. Holm, *Chem. Rev.*, 2004, **104**, 1175.
- (a) F. E. Kühn, A. D. Lopes, A. M. Santos, E. Herdtweck, J. J. Haider, C. C. Romão and A. G. Santos, *J. Mol. Catal. A: Chem.*, 2000, **151**, 147; (b) F. E. Kühn, M. Groarke,

- É. Bencze, E. Herdtweck, A. Prazeres, A. M. Santos, M. J. Calhorda, C. C. Romão, I. S. Gonçalves, A. D. Lopes and M. Pillinger, *Chem. – Eur. J.*, 2002, **8**, 2370; (c) A. Al-Ajlouni, A. A. Valente, C. D. Nunes, M. Pillinger, A. M. Santos, J. Zhao, C. C. Romão, I. S. Gonçalves and F. E. Kühn, *Eur. J. Inorg. Chem.*, 2005, 1716; (d) S. M. Bruno, B. Monteiro, M. S. Balula, C. Lourenço, A. A. Valente, M. Pillinger, P. Ribeiro-Claro and I. S. Gonçalves, *Molecules*, 2006, **11**, 298; (e) A. Günyar, M.-D. Zhou, M. Drees, P. N. W. Baxter, G. Bassioni, E. Herdtweck and F. E. Kühn, *Dalton Trans.*, 2009, 8746; (f) A. Günyar, D. Betz, M. Drees, E. Herdtweck and F. E. Kühn, *J. Mol. Catal. A: Chem.*, 2010, **331**, 117; (g) A. Günyar and F. E. Kühn, *J. Mol. Catal. A: Chem.*, 2010, **319**, 108; (h) S. M. Bruno, C. C. L. Pereira, M. S. Balula, M. Nolasco, A. A. Valente, A. Hazell, M. Pillinger, P. Ribeiro-Claro and I. S. Gonçalves, *J. Mol. Catal. A: Chem.*, 2007, **261**, 79; (i) A. C. Coelho, M. Nolasco, S. S. Balula, M. M. Antunes, C. C. L. Pereira, F. A. A. Paz, A. A. Valente, M. Pillinger, P. Ribeiro-Claro, J. Klinowski and I. S. Gonçalves, *Inorg. Chem.*, 2011, **50**, 525; (j) T. R. Amarante, P. Neves, F. A. A. Paz, A. A. Valente, M. Pillinger and I. S. Gonçalves, *Dalton Trans.*, 2014, **43**, 6059; (k) A. A. Valente, J. Moreira, A. D. Lopes, M. Pillinger, C. D. Nunes, C. C. Romão, F. E. Kühn and I. S. Gonçalves, *New J. Chem.*, 2004, **28**, 308; (l) Z. Petrovski, M. Pillinger, A. A. Valente, I. S. Gonçalves, A. Hazell and C. C. Romão, *J. Mol. Catal. A: Chem.*, 2005, **227**, 67; (m) S. Gago, J. E. Rodríguez-Borges, C. Teixeira, A. M. Santos, J. Zhao, M. Pillinger, C. D. Nunes, Z. Petrovski, T. M. Santos, F. E. Kühn, C. C. Romão and I. S. Gonçalves, *J. Mol. Catal. A: Chem.*, 2005, **236**, 1.
- 7 (a) A. Jimtaisong and R. L. Luck, *Inorg. Chem.*, 2006, **45**, 10391; (b) K. Dreisch, C. Andersson, M. Hakansson and S. Jagner, *J. Chem. Soc., Dalton Trans.*, 1993, 1045.
- 8 (a) M. D. Brown, M. B. Hursthouse, W. Levason, W. Ratnani and G. Reid, *Dalton Trans.*, 2004, 2487; (b) M. F. Davis, W. Levason, M. E. Light, R. Ratnani, G. Reid, K. Saraswat and M. Webster, *Eur. J. Inorg. Chem.*, 2007, 1903.
- 9 (a) R. J. Butcher, H. P. Gunz, R. G. A. R. Maclagan, H. K. J. Powell, C. J. Wilkins and Y. S. Hian, *J. Chem. Soc., Dalton Trans.*, 1975, 1223; (b) P. Chaumette, H. Mimoun, L. Saussine, J. Fischer and A. Mitschler, *J. Organomet. Chem.*, 1983, **250**, 291; (c) R. Sanz, J. Escribano, M. R. Pedrosa, R. Aguado and F. J. Arnáiz, *Adv. Synth. Catal.*, 2007, **349**, 713; (d) J. E. Drake, M. B. Hursthouse, M. E. Light, R. Kumar and R. Ratnani, *J. Chem. Crystallogr.*, 2007, **37**, 421; (e) S. Gago, P. Neves, B. Monteiro, M. Pessêgo, A. D. Lopes, A. A. Valente, F. A. A. Paz, M. Pillinger, J. Moreira, C. M. Silva and I. S. Gonçalves, *Eur. J. Inorg. Chem.*, 2009, 4528; (f) B. Monteiro, S. S. Balula, S. Gago, C. Grosso, S. Figueiredo, A. D. Lopes, A. A. Valente, M. Pillinger, J. P. Lourenço and I. S. Gonçalves, *J. Mol. Catal. A: Chem.*, 2009, **297**, 110.
- 10 C. D. Nunes, A. A. Valente, M. Pillinger, J. Rocha and I. S. Gonçalves, *Chem. – Eur. J.*, 2003, **9**, 4380.
- 11 F. E. Kühn, E. Herdtweck, J. J. Haider, W. A. Herrmann, I. S. Gonçalves, A. D. Lopes and C. C. Romão, *J. Organomet. Chem.*, 1999, **583**, 3.
- 12 (a) F. J. Arnáiz, R. Aguado, M. R. Pedrosa, J. Mahía and M. A. Maestro, *Polyhedron*, 2002, **21**, 1635; (b) F. J. Arnáiz, R. Aguado, M. R. Pedrosa and A. D. Cian, *Inorg. Chim. Acta*, 2003, **347**, 33; (c) N. Manwani, M. C. Gupta, R. Ratnani, J. E. Drake, M. B. Hursthouse and M. E. Light, *Inorg. Chim. Acta*, 2004, **357**, 939; (d) A. L. Bingham, J. E. Drake, M. B. Hursthouse, M. E. Light, R. Kumar and R. Ratnani, *Polyhedron*, 2006, **25**, 3238.
- 13 (a) F. J. Arnáiz, R. Aguado, J. Sanz-Aparicio and M. Martinez-Ripoll, *Polyhedron*, 1994, **13**, 2745; (b) F. J. Arnáiz, R. Aguado, M. R. Pedrosa, J. Mahía and M. A. Maestro, *Polyhedron*, 2001, **20**, 2781; (c) F. Li and G. Yuan, *Angew. Chem., Int. Ed.*, 2006, **45**, 6541; (d) Y. Luan, G. Wang, R. L. Luck and M. Yang, *Eur. J. Inorg. Chem.*, 2007, 1215.
- 14 (a) G. Wang, G. Chen, R. L. Luck, Z. Wang, Z. Mu, D. G. Evans and X. Duan, *Inorg. Chim. Acta*, 2004, **357**, 3223; (b) M. B. Hursthouse, W. Levason, R. Ratnani and G. Reid, *Polyhedron*, 2004, **23**, 1915; (c) M. F. Davis, W. Levason, R. Ratnani, G. Reid, T. Rose and M. Webster, *Eur. J. Inorg. Chem.*, 2007, 306.
- 15 T. Kottke and D. Stalke, *J. Appl. Crystallogr.*, 1993, **26**, 615.
- 16 APEX2 Data Collection Software, *Version 2.1-RC13*, Bruker AXS, Delft, The Netherlands, 2006.
- 17 Cryopad, *Remote monitoring and control, Version 1.451*, Oxford Cryosystems, Oxford, United Kingdom, 2006.
- 18 SAINT+, *Data Integration Engine, version 8.27b*, Bruker AXS, Madison, Wisconsin, USA, 1997–2012.
- 19 G. M. Sheldrick, *SADABS, version 2012/1*, Bruker AXS Area Detector Scaling and Absorption Correction, Bruker AXS, Madison, Wisconsin, USA, 2012.
- 20 G. M. Sheldrick, *SHELXT-2014, Program for Crystal Structure Solution*, University of Göttingen, 2014.
- 21 (a) G. M. Sheldrick, *Acta Crystallogr., Sect. C: Cryst. Struct. Commun.*, 2015, **71**, 3; (b) G. M. Sheldrick, *SHELXL, version 2014, Program for Crystal Structure Refinement*, University of Göttingen, 2014; (c) G. M. Sheldrick, *Acta Crystallogr., Sect. A: Found. Crystallogr.*, 2008, **64**, 112.
- 22 C. B. Hübschle, G. M. Sheldrick and B. Dittrich, *J. Appl. Crystallogr.*, 2011, **44**, 1281.
- 23 K. Brandenburg, *DIAMOND, Version 3.2f*, Crystal Impact GbR, Bonn, Germany, 1997–2010.
- 24 P. Illner, R. Puchta, F. W. Heinemann and R. van Eldik, *Dalton Trans.*, 2009, 2795.